

Experimental and numerical analysis of fatigue behaviour for tubular K-joints

Yong-Bo Shao[†] and Zhen-Bin Cao[‡]

School of Civil Engineering, Yantai University, Yantai City, 264005, P.R. China

(Received April 5, 2004, Accepted December 29, 2004)

Abstract. In this paper, a full-scale K-joint specimen was tested to failure under cyclic combined axial and in-plane bending loads. In the fatigue test, the crack developments were monitored step by step using the alternating current potential drop (ACPD) technique. Using Paris' law, stress intensity factor, which is a fracture parameter to be frequently used by many designers to predict the integrity and residual life of tubular joints, can be obtained from experimental test results of the crack growth rate. Furthermore, a scheme of automatic mesh generation for a cracked K-joint is introduced, and numerical analysis of stress intensity factor for the K-joint specimen has then been carried out. In the finite element analysis, J-integral method is used to estimate the stress intensity factors along the crack front. The numerical stress intensity factor results have been validated through comparing them with the experimental results. The comparison shows that the proposed numerical model can produce reasonably accurate stress intensity factor values. The effects of different crack shapes on the stress intensity factors have also been investigated, and it has been found that semi-ellipse is suitable and accurate to be adopted in numerical analysis for the stress intensity factor. Therefore, the proposed model in this paper is reliable to be used for estimating the stress intensity factor values of cracked tubular K-joints for design purposes.

Key words: tubular K-joints; alternating current potential drop (ACPD); stress intensity factor; J-integral; crack shapes; semi-ellipse.

1. Introduction

Tubular K-joints are widely encountered in the offshore platforms, bridges and railways as supporting structures. These joint structures are frequently subjected to cyclic loads caused by wind and seawater. Hence, fatigue failure becomes a very common phenomenon. It has been found that the surface crack always initiates at the hot spot stress region caused by curvature discontinuity or initial defect at the weld after the joints are subjected to a number of cyclic loads. The initiation of the surface crack at the weld will reduce the ultimate strength and the supporting capacity of these joints. Thus, it is crucial to be able to estimate the residual life of these cracked joints. For a joint without initial crack, the most commonly used method to estimate how many cycles this joint can sustain is to refer to an S-N curve (Zhao *et al.* 2001). When a K-joint is subjected to certain loading conditions, the hot spot stress range can be obtained from finite element analysis or experimental

[†] Lecturer, Corresponding author, E-mail: cybshao@ytu.edu.cn

[‡] Associate Professor

test. The number of cycles can then be predicted from the S-N curve based on the hot spot stress range. Therefore, the fatigue life of this joint can be estimated in practice. However, this method is only suitable for uncracked K-joints. That means if a K-joint has an initial crack, S-N curve can no longer be adopted for estimating the remaining life of the damaged joint. An alternative method is to use fracture mechanics approach, based on accurate estimation of stress intensity factors, to calculate the residual life of such damaged joints.

To analyze the stress intensity factor of a cracked tubular K-joint, the details of the crack developments must be obtained before numerical analysis. Therefore, it is necessary to investigate the crack developing behaviour of the K-joint subjected under fatigue load. Generally, K-joints are mainly subjected to combined load. In practice, in-plane bending and axial loads are two dominant loads for tubular K-joints. In case of this combined loading condition, surface crack usually initiates at the crown position on the chord and propagates along the weld curve to the saddle. In fatigue test for tubular joints, it is easier to measure the crack length in the process of crack propagation. However, it is extremely difficult to monitor the accurate information of crack depth during crack propagating. Alternating current potential drop (ACPD) technique is then used to monitor the crack shape developments step-by-step through the test for a K-joint in this study.

Up to now, there are very few published stress intensity factor results in the literature for tubular K-joints. Although some fatigue tests have been carried out on some tubular joints, nearly all the specimens used in these tests are small-scale. Fatigue tests on large-scale tubular joints have scarcely reported, especially for K-joints. Furthermore, all the previous experimental tests on tubular joints only measured the crack length developments. The crack depth developments in these fatigue tests have not been captured.

In numerical analysis of the stress intensity factor, mesh generation of the surface crack is critical. Therefore, five types of elements, i.e., hexahedral, prism, quarter-point collapsed prism, tetrahedron and pyramid elements, are used to model the surface crack and other zones of the K-joint in this study. Different types of elements can control element density and aspect ratio easily to assure that the generated mesh is of high quality. Additionally, in numerical analysis of the stress intensity factor, surface crack shape is assumed to be semi-elliptical by most researchers although the actual crack shape may be not very close to it. The effects of different crack shapes on the stress intensity factor values have been investigated in this study. Numerical stress intensity factor results have been validated through comparing them to the experimental test results.

2. Experimental tests on a large-scale K-joint specimen

2.1 The specimen and the test rig

The configuration of the test specimen is illustrated in Fig. 1. The specimen was fabricated from circular hollow sections. The chord and the braces were fabricated by using steel pipes according to API 5L Grade B specifications (American Petroleum Institute 1993). The yield stress and ultimate stress of the steel material are 302 MPa and 494 MPa respectively. The weld size of the specimen is accordance with American Welding Society (AWS) Structure Welding Code D1.1-96 (1996) specification. After fabrication, the weld profile was checked using ultrasonic technique to ensure the welding quality is acceptable. At both ends of the chord, thick plates were welded to provide fixed boundary conditions. For the brace of a shorter length, a plate was also welded to fix the end

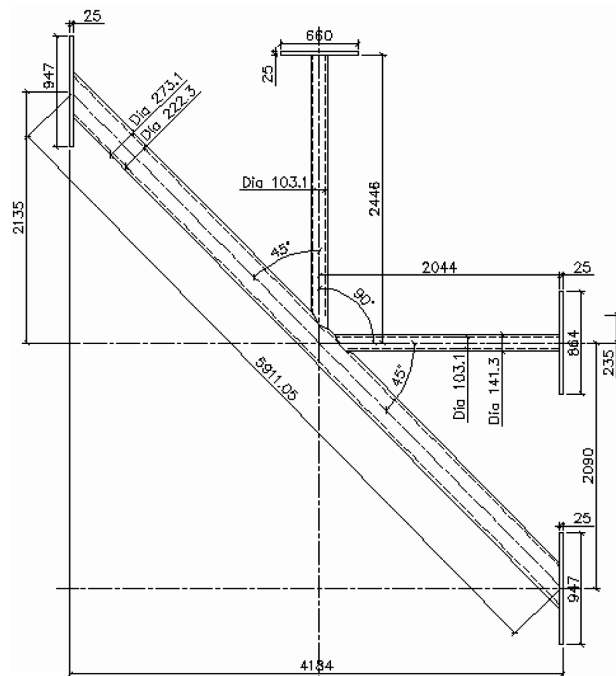


Fig. 1 Configuration of the K-joint specimen

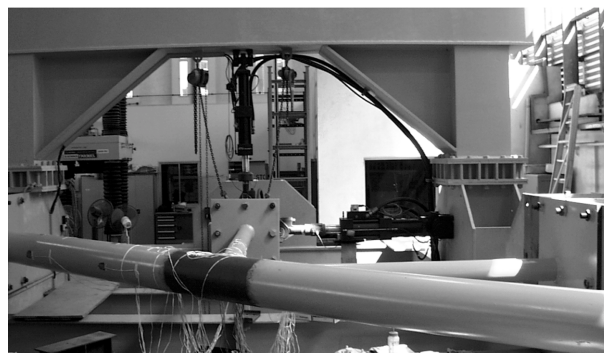


Fig. 2 View of a specially designed test rig

of the brace. In experimental test, external loads were applied in the end of the brace of a longer length.

A specially designed test rig, as shown in Fig. 2, was used to conduct the test. The rig can provide loads in three mutually perpendicular directions by controlling three hydraulic actuators. Basic load can be applied by using any actuator individually. Two or three actuators can supply loads spontaneously to provide combined load conditions.

2.2 Static test

For tubular K-joints subjected to cyclic load, fatigue crack generally generates at the position of

peak hot spot stress. The location and the magnitude of the peak hot spot stress determine the crack development and propagation, and hence they are significantly important for estimating the fatigue life. Therefore, static test is necessary to be carried out to locate the stress distribution along the weld on the chord and on the brace before fatigue test.

Strain gauges are generally used to measure the strain distribution along the weld. At each spot around the weld, two strain gauges placed in an extrapolation region are used to measure the strains perpendicular to the weld curve. The two strain gauges are placed in the range of extrapolation region specified in CIDECT (Zhao *et al.* 2001). Then the strains at the weld toe can be obtained using linear extrapolation method, and the stresses at the weld toe are then obtained from the relationship between stress and strain.

The two strain gauges placed perpendicular to the weld are used to measure the strains perpendicular to the weld (ξ_{\perp}). At some critical positions, such as crown, heel and saddle etc., two additional strain gauges are placed parallel to the weld curve. These strain gauges are used to measure the strains parallel to the weld (ξ_{\parallel}). A close view of the strain gauges can be seen in Fig. 3. After the strains at the weld toe were obtained by linear extrapolation method, the stresses can be obtained from the following equation:

$$\sigma_{HSS} = \varepsilon_{HSS} \times (1 + \nu \cdot \xi_{\parallel} / \xi_{\perp}) / (1 - \nu^2) = c \cdot \varepsilon_{HSS} \quad (1)$$

where σ_{HSS} is the hot spot stress and ε_{HSS} is the hot spot strain. ν is Poisson's ratio. c is a coefficient which is generally between 1.1-1.2. The coefficient c is determined from the strains ξ_{\perp} and ξ_{\parallel} measured in the static experimental test.

In the static test, the specimen was tested under combined axial and in-plane bending loads. The applied axial load is 180.0 kN and the in-plane bending load is 18.0 kN. The obtained stress distributions for the chord and for the brace are illustrated in Fig. 4. It is clear that the peak hot spot stress is located at the crown position on the chord. The stress along the weld is nearly symmetrical. The peak hot spot stress on the chord is about 250.0 MPa.

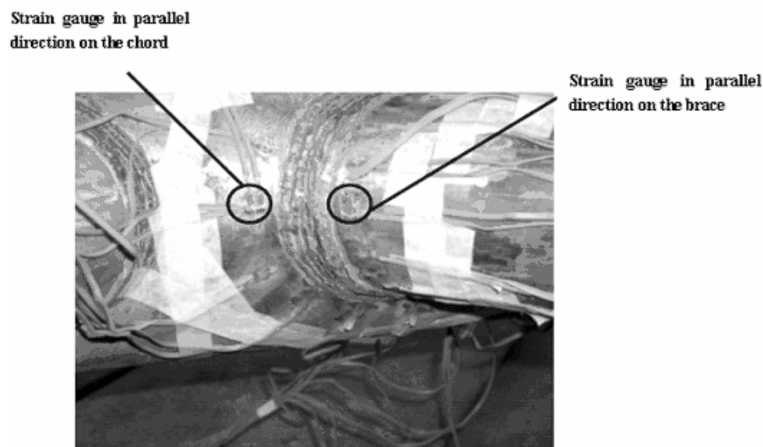


Fig. 3 Close view of the strain gauges

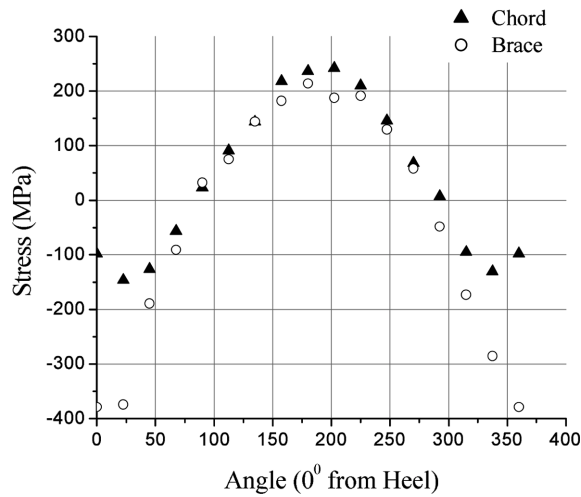


Fig. 4 Stress distribution along the weld curve on chord and on brace

2.3 Fatigue test

The fatigue test was conducted in air under combined axial and in-plane bending loads till failure by using the test rig shown in Fig. 2. Both the axial and the in-plane bending loads, as seen in Fig. 5, are sinusoidal constant amplitude loads. The stress ratio, R , is equal to zero and a frequency of 0.2 Hz was used throughout the fatigue test.

To monitor the crack developments during the fatigue test, ACPD technique is used in present study. This technique has been proved to be effective to measure the crack profiles in fatigue test (Huang 2002). The concept of ACPD can be illustrated in Fig. 6. ACPD uses an alternating current with a high frequency of about 5.0 kHz, which is induced on the surface of ferromagnetic material. When the current passes through a conductor, the so-called “skin-effect” δ forces the current to flow in a thin layer on the outer surface. Materials of high permeability and conductivity have small skin

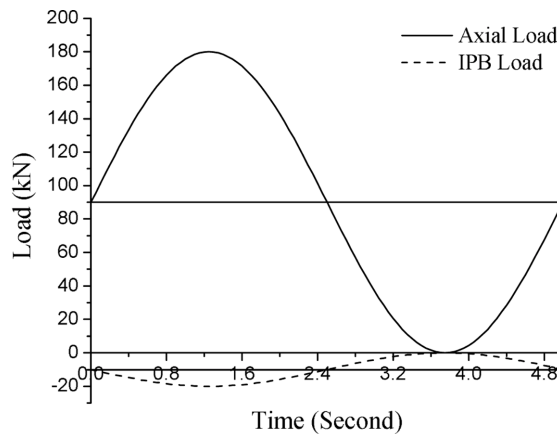


Fig. 5 Cyclic loads in fatigue test

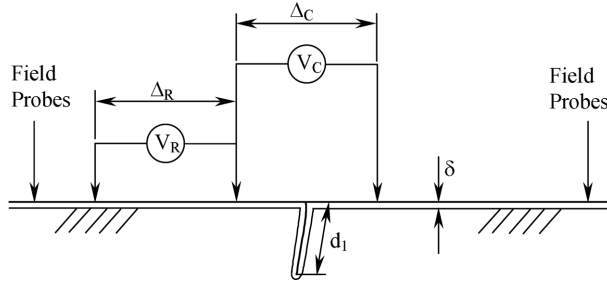


Fig. 6 ACPD theory and notation

depth. For example, at a frequency of 5.0 kHz, ferromagnetic mild steel has a skin depth of the order of 0.1 mm. When an alternating current flows across a surface with a crack, the current will flow down on crack side and up the other side. A linear potential gradient is assumed to exist in the metal surface and on crack surfaces. As seen in Fig. 6, a surface crack lies in gap Δ_C and gap Δ_R is taken as a reference gap. Then the relationship between the potential drop and the gap can be expressed as follow:

$$V_C \propto \Delta_C + 2d_1$$

$$V_R \propto \Delta_R \tag{2}$$

When $\Delta_C = \Delta_R = \Delta$, crack depth d_1 can be obtained as follow:

$$d_1 = \frac{\Delta}{2}(V_C/V_R - 1.0) \tag{3}$$

In the fatigue test, probes were equally spaced every 10 mm around the connection at the hot spot site. The arrangements of the probes are illustrated in Fig. 7. A U10 Crack Microgauge (TSC 1991) was connected to these probes. The ACPD can monitor a crack accurately if its length is less than 310 mm because 32 sites were spotted along the weld curve.

From the fatigue test result, it has been found that the surface crack initiates at the crown position

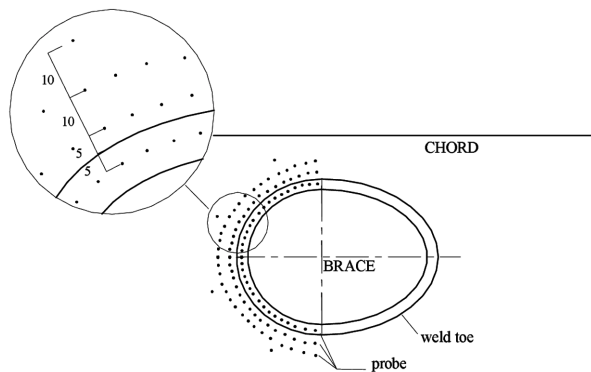


Fig. 7 Plan view of the probe sitting

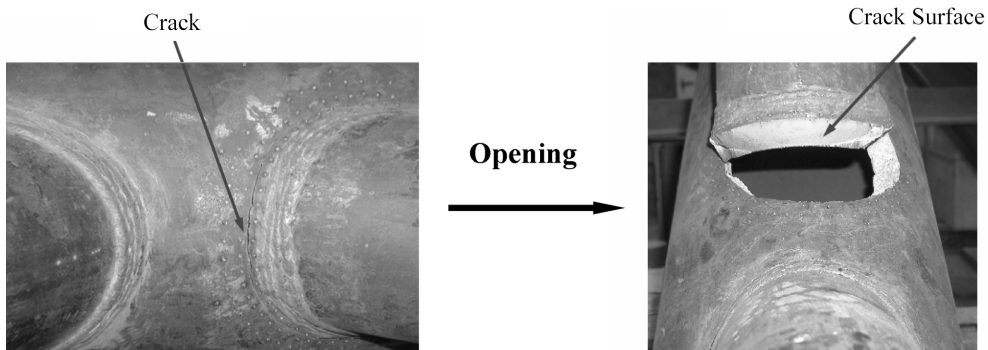


Fig. 8 Surface crack at the crown

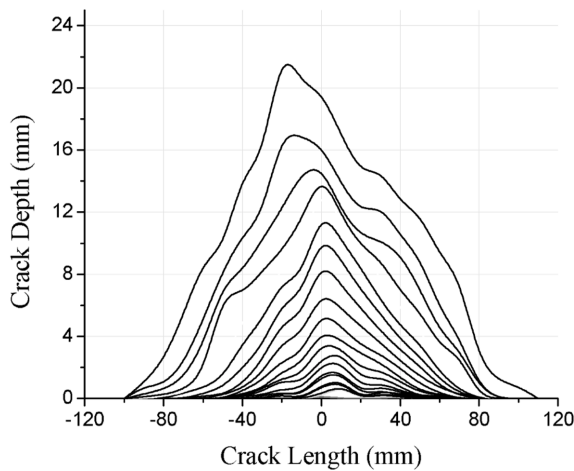


Fig. 9 Crack development curves with an interval of 10000 cycles

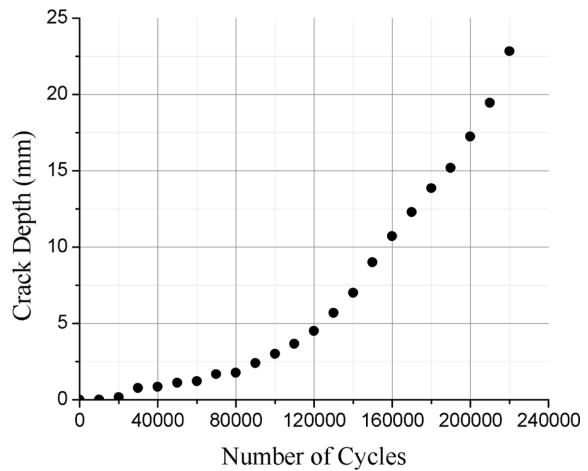


Fig. 10 Crack growth at the deepest point

and propagates to the saddle very symmetrically. Figs. 8(a) and 8(b) show the surface crack after the fatigue test. From Fig. 8(a), it has been found that the surface crack is nearly symmetrical to the crown position. Fig. 8(b) shows a detailed surface crack after the specimen was splitted into two parts. It has been found that the some crack shapes can be measured manually because there are several striations in the crack surface. Therefore, some crack depths can be measured manually from the crack surface of the specimen. The observation of the starting point of the crack agrees well with speculation from static test of the hot spot stress distribution. The crack development was monitored and recorded during the fatigue test. The details of the crack profile every 10000 cycles are plotted in Fig. 9. It can be seen that the deepest point is almost kept constant in the process of crack propagation. The crack growth rate at the deepest point is depicted in Fig. 10.

In most numerical analysis for cracked tubular joints, semi-ellipse is adopted as the surface crack shape. In this test, the actual crack shape can be measured manually after the specimen was splitted into two parts. As shown in Fig. 8(b), it has been found that some crack striations are clear in the crack surface. Therefore, some crack profiles can be measured by hand. The comparison of different crack profiles is illustrated in Fig. 11. Apparently, actual crack shape is not exactly a semi-ellipse.

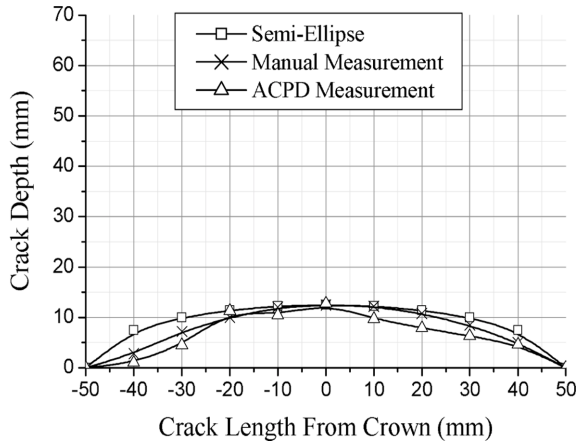


Fig. 11 Comparison of different crack shapes

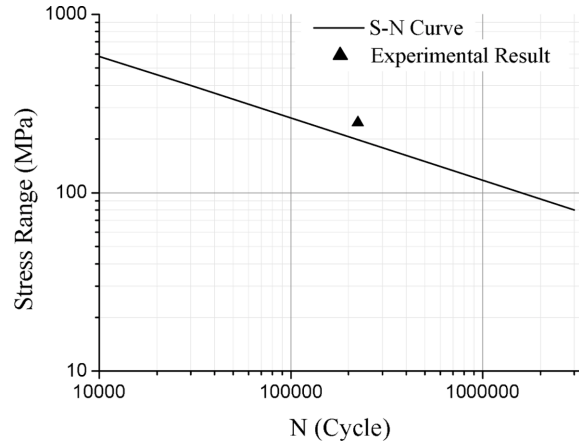


Fig. 12 S-N data from experimental test

Especially at the region near the two crack tips, the measured shape is much different with a semi-ellipse. It can be seen that ACPD readings can provide accurate information of crack depth along the crack front at some sites. In some sites near the crack tips, ACPD readings can not provide accurate crack depth. However, at the deepest point, ACPD readings can always provide acceptably accurate size for the crack depth.

The hot spot stress range can be used for predicting the service life of tubular joints under cyclic load from an S-N curve. For this test, the predicted life from an S-N curve and the experimental test result are compared and the comparison is plotted in Fig. 12. The experimental result shows that S-N curve proposed by CIDECT (Zhao *et al.* 2001) is safe but conservative to be used for estimating the entire service life of uncracked tubular joints. It should be noted that the definition of fatigue failure is very important since the number of loading cycles is the assessment parameter of failure. In this paper, the definition of fatigue failure for tubular joints is provided by DEn (1993). The fatigue failure is that “first through wall cracking detected either visually or more accurately noting loss of internal pressure or by monitoring of strain gauges positioned adjacent to the deepest part of the crack”. Therefore, when the crack just penetrates the wall thickness, the tubular joint is thought to be in failure. This definition is reasonable for tubular joints because in this stage, the penetrating crack will cause the tube structure to be submerged into seawater and reduce the internal pressure in the chord or brace member although the structure may be still able to sustain the external loadings.

3. Numerical analysis of cracked K-joints

In the finite element analysis for cracked K-joints, stress intensity factor is a useful parameter used to predict the remaining life of tubular K-joints with a surface crack. In the finite element analysis of stress intensity factor, J-integral is commonly used. J-integral is a measure of strain energy in the region of crack tip. The advantage of J-integral is that it is insensitive to mesh refinement. This is especially useful in numerical analysis because it is extremely difficult to produce good quality mesh in the region near the crack tips. However, crack mode in tubular joints is complicated and generally presented as mixed mode (DEn 1993, Bowness and Lee 1995). J-

integral can not be used directly to mixed mode problem. To solve this problem, Shih and Asaro (1988), Bowness and Lee (1996) proposed another relationship between J-integral and the stress intensity factor. The relationship is expressed as follow:

$$J = \frac{1}{8\pi} \mathbf{K}^T \cdot \mathbf{B} \cdot \mathbf{K} \quad (4)$$

where \mathbf{K} is the stress intensity factor matrix and $\mathbf{K} = [K_1, K_2, K_3]^T$, and \mathbf{B} is called the pre-logarithmic energy factor matrix. For homogenous, isotropic material, \mathbf{B} is a diagonal matrix. In this case, Eq. (4) can be reduced to the following expression:

$$J = \frac{1}{\bar{E}}(K_1^2 + K_2^2) + \frac{1}{2G}K_3^2 \quad (5)$$

where $\bar{E} = E$ for plane stress and $\bar{E} = E/(1 - \nu^2)$ for plane strain, axisymmetry and 3-D problems. G is shear modulus.

Although Eq. (5) indicates the relationship between the J-integral and the stress intensity factor, K_1 , K_2 and K_3 can not be obtained from J-integral directly. Shih and Asaro (1988), Bowness and Lee (1996) then proposed an interaction integral method to analyze mixed crack mode problem. From this method, the stress intensity factor can be achieved from the following equation:

$$J = 4\mathbf{KB} \cdot \mathbf{J}_{int} \quad (6)$$

where \mathbf{J}_{int} is the interaction integral. The details calculations of \mathbf{J}_{int} are provided in Bowness and Lee (1996).

3.1 Mesh generation scheme

Mesh quality of the surface crack has critical effects on the stress intensity factor for tubular K-joints in numerical analysis. Many past works have proved that what types of elements are used would affect the stress intensity factor results very much. Bowness and Lee (1995), DEn (1993) had used prism singular elements to model the crack front and used 3-D hexahedral elements to model the volume far away from the crack. Cao *et al.* (1997), Shih and Asaro (1988) also adopted a similar approach to model a T-joint with a surface crack. However, the results were not very accurate as the aspect of the elements near the crack front is very large. The elements near the crack were badly distorted because only two types of elements could not simulate the crack for the limited choice. This means it is impossible to get good quality elements if only two types of elements are used. Therefore, in present study, five types of elements, named hexahedral, prism, tetrahedral, pyramid and quarter-point crack elements, are adopted in this study. All the five types of elements are used to model the surface crack at the weld. In the region far away from the surface crack, only hexahedral elements are used.

As mentioned previously, the modelling of the surface crack is the critical aspect in analysis of the stress intensity factor for cracked K-joints. Fig. 13 shows the mesh of a surface crack which is extracted from the weld. As illustrated in Fig. 13, the elements in the first ring are quarter-point crack tip elements which consist of the crack front. The second ring is consisted of prism elements, which are used to connect the crack elements and pyramid elements. SFBLOCK-A, which is to connect with solid elements, is consisted of pyramid, prism and tetrahedral elements. It is a

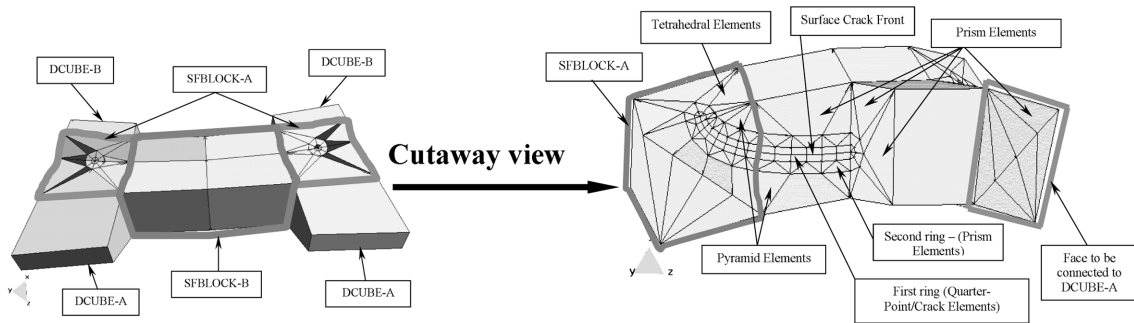


Fig. 13 Mesh of surface crack

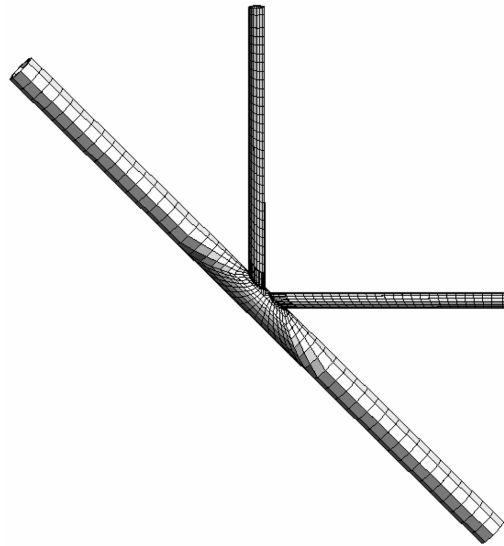


Fig. 14 Mesh of the K-joint specimen

transition zone. However, as different types of elements are used in this zone, the incompatibility of the surface becomes a big problem when merge the block to the weld. Because of this reason, tetrahedral and pyramid elements are used in DCUBE-A and DCUBE-B. These two blocks are used to link the side faces of block SFBLOCK-A.

The mesh of the entire structure of the experimental specimen can be seen in Fig. 14. In order to study the convergence of the numerical stress intensity factor results of the K-joints, one uniform refinement is carried out by improving the mesh density. Finite element meshes with refinement can be obtained by first increasing the order of a linear mesh to generate a quadratic, and then subdividing the high order elements into a number of linear elements. For example, a *parent* 8-node hexahedral element can be doubled by first converted it to a quadratic element and then subdivide the high order element to eight 8-node hexahedral elements. Obviously, other 3D elements can also be divided in a similar manner to double the density of the mesh. Note that during mesh doubling, the 5-nodes pyramid element will be divided to six 5-node pyramid and four 4-node tetrahedral elements instead of eight 5-node pyramid elements. Such division schemes will ensure the compatibility at the element interfaces when different elements are joined to a 5-node pyramid

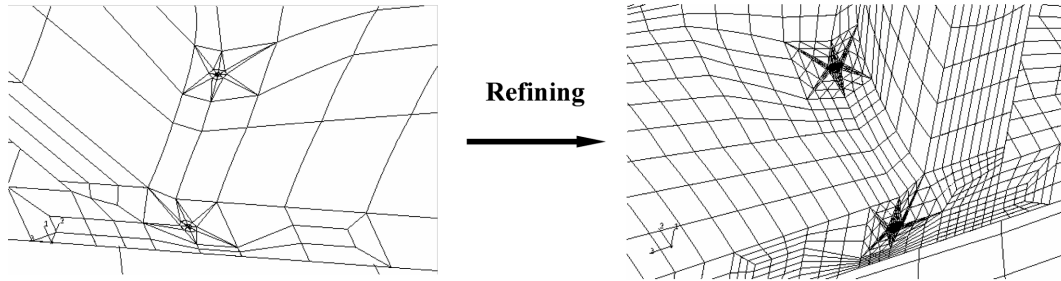


Fig. 15 Section view of a surface crack

element. This element order and density increasing schemes are applied to the mesh generation problem of cracked tubular K-joints to verify the convergence of the stress intensity factor values. The mesh refinement can be seen in Fig. 15.

3.2 Numerical analysis of stress intensity factor

The crack developments of the specimen have been monitored and the crack shapes can be determined from ACPD readings. Consider the joint with a crack of length $2c = 126$ mm and depth $d = 13.5$ mm, which was obtained from the recorded data in the fatigue test. J-integral is used to calculate the stress intensity factor of this model. The specimen is subjected to a combination of axial (180.0 kN) and in-plane bending (18.0 kN) loads. Fixed boundary conditions were provided in both ends of the chord and one end of the brace of shorter length. The finite element results of K_1 , K_2 and K_3 are plotted in Fig. 16. Fig. 16 shows that K_1 is dominant in the mixed mode, and K_2 and K_3 are much smaller compared to K_1 . To consider the effects of K_2 and K_3 , an equivalent stress intensity factor, K_e , is proposed here. The definition of K_e was proposed by Chong Rhee *et al.* (1991), Cao *et al.* (1997) and is expressed as follow:

$$K_e = [K_1^2 + K_2^2 + K_3^2 / (1 - \nu^2)]^{1/2} \tag{7}$$

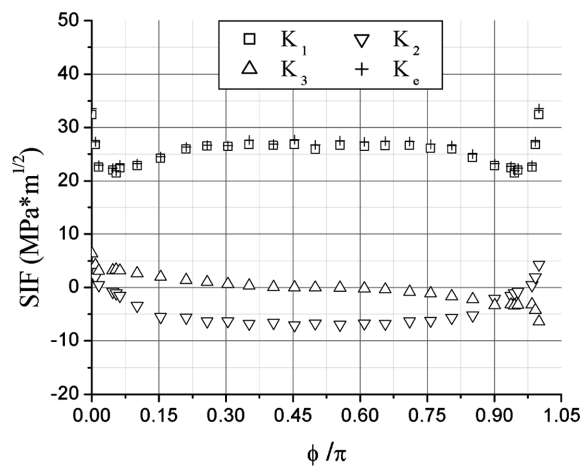


Fig. 16 Numerical results of SIF

The values of K_e are also plotted in Fig. 16. The results show that K_1 is much closer to K_e . This means for tubular K-joints under combined axial and in-plane bending loads, K_1 is more important than K_2 and K_3 . The crack mode is mainly expressed as opening mode.

3.3 Validation of stress intensity factor results

The accuracy of the numerical stress intensity factor values can be validated by the experimental test results. In the fatigue test, the stress intensity factor is obtained from Paris' law expressed as follow:

$$\frac{da}{dN} = C(\Delta K)^m \quad (8)$$

where N is the number of cycles, C and m are material constants. The values of C and m are provided by material supplier and $C = 1.45 \times 10^{-11}$ (m/cycle)(MPa*m^{1/2})^{-2.75}, $m = 2.75$. ΔK is the stress intensity factor range.

In the fatigue test, crack depth rate da/dN was obtained from ACPD readings. Then the stress intensity factor values of different crack depths can be calculated from Eq. (8). Numerical results and experimental test results are all plotted in Fig. 17. Apparently, it seems numerical analysis can provide accurate predictions for the stress intensity factor values during crack propagation. The maximum error is about 10%.

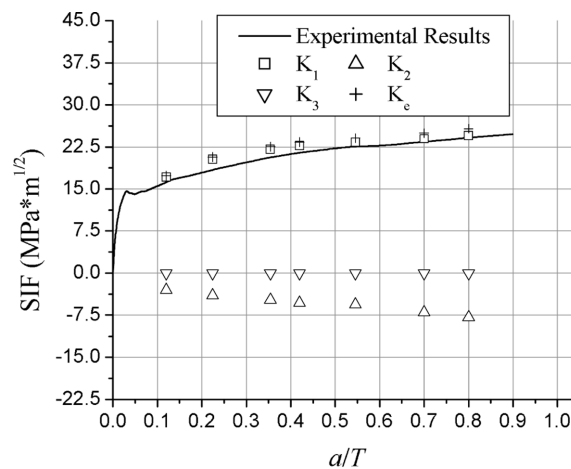


Fig. 17 SIF results for the specimen

3.4 Effects of crack shapes on stress intensity factor

In the above finite element analysis, semi-ellipse is used as the surface crack shape. As shown in Fig. 11, the actual crack shape is not very like a semi-ellipse at the two crack tips. Therefore, the effects of different crack shapes on the stress intensity factor values must be investigated. In Fig. 18, different crack shapes are plotted, and they are used to do numerical stress intensity factor computation.

The different stress intensity factors are then obtained and plotted in Fig. 19. It is clear that semi-

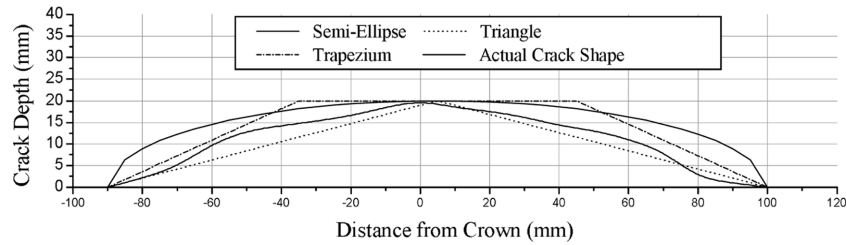


Fig. 18 Comparison of different crack shapes

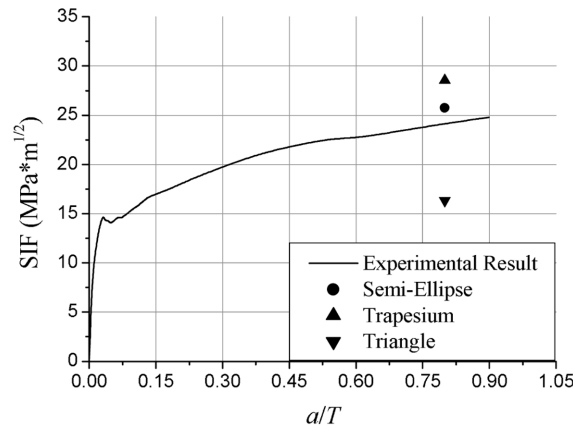


Fig. 19 Comparison of the SIF results obtained from different crack shapes

ellipse can produce accurate estimation for the stress intensity factor values. However, the stress intensity factors obtained from trapezium shape and triangle shape are much different compared with the experimental test results. This means semi-ellipse is a better choice for crack shape in analysis of the stress intensity factor for cracked K-joints.

4. Conclusions

In this paper, an experiment on a large-scale tubular K-joint specimen was conducted. Static test was first carried out to locate the hot spot stress along the weld for the K-joint specimen under combined axial and in-plane bending loads. Thereafter, the fatigue test was conducted to study the behaviour of the K-joint subjected under cyclic load. Alternating current potential drop (ACPD) technique was used to monitor crack initiation and development along the weld curve during the fatigue test. The crack profile was then obtained and the crack propagating process was simulated. Experimental test has shown that the service life of the K-joint specimen estimated from the S-N curve is safe and conservative.

Numerical analysis then has been carried out to analyze the stress intensity factor, which is critical in predicting the remaining life of a cracked K-joint. Numerical results agree very well with experimental results. Different crack shapes have been analyzed and the effects of different crack shapes on the stress intensity factor results show that semi-ellipse is suitable to be adopted in finite element analysis of the stress intensity factor values for cracked tubular K-joints.

References

- American Petroleum Institute (1993), *Recommended Practice for Planning, Designing and Constructing Fixed Offshore Platforms*. American Petroleum Institute, Washington, DC, API.
- American Welding Society (1996), *ANSI/AWS D1.1-96 Structural Welding Code-Steel*. Miami, USA.
- Bowness, D. and Lee, M.M.K. (1995), "The development of an accurate model for the fatigue assessment of doubly curved cracks in tubular joints", *Int. J. Fracture*, **73**, 129-147.
- Bowness, D. and Lee, M.M.K. (1996), "Stress intensity factor solutions for semi-elliptical weld-toe cracks in T-butt geometries", *Fatigue Fract. Engng Mater. Struct.*, **19**(6), 787-797.
- Cao, J.J., Yang, G.J. and Packer, J.A. (1997), "FE mesh generation for circular tubular joints with or without cracks", *Proc. 7th Int. Offshore and Polar Eng. Conf.*, Honolulu, **6**, 98-105.
- Chong Rhee, H., Han, S. and Gipson, G.S. (1991), "Reliability of solution method and empirical formulas of stress intensity factors for weld toe cracks of tubular joints", *Proc. 10th Offshore Mechanics and Arctic Eng. Conf.*, ASME, **3**(B), 441-452.
- Department of Energy (DEn), (1993), "Background to new fatigue design guidance for steel joints in offshore structures", *Internal Report*, London, UK.
- Huang, Z.W. (2002), "Stress intensity factor of cracked steel tubular T and Y-joints under complex loads", PhD Thesis, Nanyang Technological University, Singapore.
- Shih, C.F. and Asaro, R.J. (1988), "Elastic-plastic analysis of cracks on bimaterial interfaces: Part I – Small scale yielding", *J. Appl. Mech.*, 299-316.
- Technical Software Consultant Ltd. (TSC) (1991), *ACFM Crack Microgauge – Model U10*, Milton Keynes, UK.
- Zhao, X.L., Herion, S., Packer, J.A., Puthli, R., Sedlacek, G., Wardenier, J., Weynand, K., van Wingerde, A. and Yeomans, N. (2001), *Design Guide for Circular and Rectangular Hollow Section Joints under Fatigue Loading*. CIDECT, TUV.